Published in final edited form as:
Reprod Toxicol. 2014 June ; 45: 59–70. doi:10.1016/j.reprotox.2014.01.006.

Sub-acute intravenous administration of silver nanoparticles in male mice alters Leydig cell function and testosterone levels

THOMAS X. GARCIA[1,2], **GUILHERME M. J. COSTA**[3], **LUIZ R. FRANÇA**[3], and **MARIE-CLAUDE HOFMANN**[1,2]

[1]Department of Comparative Biosciences, University of Illinois at Urbana-Champaign, Urbana, IL 61802, USA

[2]Department of Endocrine Neoplasia and Hormonal Disorders, The University of Texas MD Anderson Cancer Center, Houston, Texas, USA

[3]Laboratory of Cellular Biology, Department of Morphology, Federal University of Minas Gerais, Belo Horizonte, Minas Gerais, Brazil

Abstract

The aim of this study was to determine whether short-term, *in vivo* exposure to silver nanoparticles (AgNPs) could be toxic to male reproduction. Low dose (1 mg/kg/dose) AgNPs were intravenously injected into male *CD1* mice over 12 days. Treatment resulted in no changes in body and testis weights, sperm concentration and motility, fertility indices, or follicle-stimulating hormone and luteinizing hormone serum concentrations; however, serum and intratesticular testosterone concentrations were significantly increased 15 days after initial treatment. Histologic evaluation revealed significant changes in epithelium morphology, germ cell apoptosis, and Leydig cell size. Additionally, gene expression analysis revealed *Cyp11a1* and *Hsd3b1* mRNA significantly upregulated in treated animals. These data suggest that AgNPs do not impair spermatogonial stem cells *in vivo* since treatment did not result in significant decreases in testis weight and sperm concentrations. However, AgNPs appear to affect Leydig cell function, yielding increasing testicular and serum testosterone levels.

Keywords

testis; spermatogenesis; reproductive toxicity; fertility

Address for correspondence: Marie-Claude Hofmann, PhD, Department of Endocrine Neoplasia and Hormonal Disorders, The University of Texas MD Anderson Cancer Center, 1515 Holcombe Boulevard, Unit 1105, Houston, Texas 77030, USA, Phone: 1-713-745-2009, Fax: 1-713-794-4065, mhofmann@mdanderson.org.

1. Introduction

Spermatogonial stem cells (SSCs) provide the foundation for spermatogenesis through their ability to both self-renew and generate daughter cells, which differentiate into spermatozoa. These characteristics make SSCs vital for the maintenance of male fertility and the perpetuation of the species. The complex biological processes underlying spermatogenesis are particularly sensitive to environmental insults [1]. Many chemicals and ultrafine particles have been shown to have a detrimental effect on the testes, either directly, by affecting the germ cells, or indirectly, by acting on the somatic cells [2, 3].

Nanoparticles (NPs) have been shown to easily traverse biological membranes such as those across epithelia and the walls of very small capillaries. Thus, following exposure or systemic administration, NPs can easily move throughout the body, potentially affecting any number of different tissues [4-6]. For example, in addition to passing through the blood-brain barrier [7-9], NPs have been shown to penetrate the blood-testis barrier and reach the seminiferous epithelium [5]. NP-related damage to the brain has been shown [9], but few studies have focused on the effect of NPs on the testes.

Among these detrimental substances are silver nanoparticles (AgNPs), which typically range in size from 1 to 100 nm and have become one of the most commonly used nanomaterials in consumer products mostly due to its antibacterial properties. AgNPs may be found as components of bandages, clothing, cosmetics, car wax, toys, and antistatic materials [10, 11]. Several previous reports have shown that AgNPs have negative effects on somatic cell lines *in vitro* [12-16]. *In vivo* studies have also shown AgNP-related injuries to the brain, liver, and lung [9, 17, 18]. AgNPs are additionally a concern for male fertility because they have been found to reach the testes after administration [19-21].

Recently, several studies described the effects of subchronic oral or inhalation toxicity of AgNPs in rodents [19, 20]. In each of those studies, the accumulation of silver was observed in the blood and all tested organs, including the liver, spleen, kidneys, thymus, lungs, heart, brain, and testes. To our knowledge, however, no study described the effect of AgNPs on fertility, sex hormone production, or live sperm output and performance.

Recent studies from our lab examined the *in vitro* effects of AgNPs on the mouse spermatogonial stem cell (SSC) line, C18-4, at the molecular level [22-24]. Our data showed that AgNPs interfere with SSC proliferation in a dose-dependent (μg particles per ml culture medium) and particle size-dependent manner and that small AgNPs (10-25 nm in diameter) are more likely than larger sized AgNPs (80-130 nm in diameter) to promote apoptosis or the production of reactive oxygen species in these cells. In addition, our data demonstrated that AgNPs are able to disrupt components of the glial cell-derived neurotrophic factor (GDNF) signaling pathway, a pathway essential for self-renewal of SSCs *in vitro* and *in vivo*. Our data revealed that at a concentration of 10 μg/ml, AgNPs specifically interacted with and inhibited the activity of Fyn kinase downstream of GDNF, thereby inhibiting SSC proliferation *in vitro*. These acute *in vitro* effects of AgNPs, if recapitulated *in vivo*, would be deleterious to male fertility.

In vitro studies have established a direct link between AgNPs and SSC toxicity [22, 23], and *in vivo* studies have demonstrated the ability of NPs to penetrate the testes and/or negatively affect testis function [5, 8, 19, 20, 25-28]. Based on our previous *in vitro* data [23], we hypothesized that AgNPs could directly influence SSC activity *in vivo*, thereby negatively affecting sperm production and fertility. To test this, we administered AgNPs (1 mg/kg/day or 0 mg/kg/day control) intravenously to male mice 5 times over a 12-day period and assessed AgNPs' effect on fertility, sex hormone production, testis histology, and sperm output. Administration of AgNPs resulted in changes in testis histology, increases in serum and intratesticular testosterone, and increases in intratesticular *Cyp11a1* and *Hsd3b1* gene expression. However, AgNPs did not affect sexual behavior, body and testis weights, sperm concentration and motility, or fertility as assessed by pregnancy rate, number of implantations, and gestational survival. Therefore, AgNPs do not appear to be toxic to germline stem cells *in vivo* at the concentration and duration of exposure tested, but our results demonstrate that AgNPs have the potential to significantly alter steroid production and impact testis health.

2. Methods

2.1. Silver nanoparticles

Citrate-coated AgNPs of approximately 10 nm size were purchased from nanoComposix, Inc. (San Diego, CA, US) at a supplied stock concentration of 1.00 mg/ml. The AgNP size distribution after 1:10 dilution of stock nanomaterial in phosphate buffered saline (PBS) was measured by dynamic light scattering (DLS; Brookhaven Instruments, Model #, Holtsville, NY), and the mean diameter was found to be 14 nm (Fig. 1A). Additionally, the size and morphology was assessed through transmission electron microscopy (TEM; Fig. 1B).

2.2. Transmission Electron Microscopy of AgNPs

One drop of stock nanoparticle solution diluted 1:10 in PBS was placed on a formvar plastic and carbon-coated copper grid that was placed atop of a small piece of Parafilm. Excess sample was removed with filter paper and the grid was submerged in a solution of 2% ammonium molybdate for 2 minutes. Excess fluid was again removed using filter paper, and the grid placed into a grid box, which was then covered with drierite desiccant crystals for 10 minutes. The grid was then examined and photographed with a Hitachi H600 Transmission Electron Microscope at 20,000x or higher magnification.

2.3. Mice

Male and female *CD1* mice (4-5-weeks old) were obtained from Charles River Laboratories (Wilmington, MA, US) and maintained in the animal facilities of the College of Veterinary Medicine at the University of Illinois Urbana-Champaign and the Institute for Biosciences and Technology, Texas A&M Health Science Center. At both facilities mice were housed at 25 °C with a 12 hour light, 12 hour dark photoperiod and given tap water and a standard rodent chow diet. All animal experiments were approved by the Institutional Animal Care and Use Committee (IACUC) at the University of Illinois Urbana-Champaign and the Institute for Biosciences and Technology, Texas A&M Health Science Center, and all experiments were conducted in accordance with the National Institute of Health Guide for

the Care and Use of Laboratory Animals. Prior to administration of the first dose, mice were acclimated for 1 week. In sum, 60 males were randomly divided into 5 sets of 12 mice each, and each set of 12 mice were randomly divided into two separate cohorts: vehicle (control group) and 1 mg/kg AgNP (per dose) treated. Each set was used for the different time points and analyses as discussed below. The concentration of 1 mg/kg was chosen to achieve serum concentrations roughly equivalent to the lowest *in vitro* dose found with effects in our previous studies, 10 μg/ml [23].

Nanoparticle suspensions were freshly prepared for each animal exposure by diluting stock nanoparticle solution 1:10 in phosphate buffered saline (PBS), pipetting up and down, and then immediately injecting into the tail veins of treated mice. Particles were diluted in PBS to obtain a physiological solution suitable for intravenous injection and no agglomeration was observed visually or through DLS analysis during the short (approximately 0.5-2 minute) duration between dilution and injection (or DLS analysis). Control mice were given an equivalent amount of PBS containing a 1:10 dilution of 2 mM citrate buffer via the tail vein. Mice were given 5 injections (1 injection every 3 days on days 0, 3, 6, 9, and 12) (Fig. 2).

Two sets of control and treated mice were utilized for isolation at 15 days post-initial treatment: one set for the isolation of testes for ICP-MS analysis and the other for all other tissue processing. An additional 3 sets of control and treated mice were used for breeding assessment beginning at days 15, 60, and 120 post-initial treatment. Those animals whose breeding assessment was carried out at 15 and 60 days were subsequently used for isolation at 60 and 120 days, respectively.

Mice were sacrificed by CO_2 asphyxiation, and blood, cauda epididymis, and testis samples were collected. Serum samples were obtained from blood by clotting at room temperature for 30 minutes, followed by centrifugation at 1,000 g for 10 minutes. The right cauda epididymis was processed for sperm analysis as described below, and testes were collected, weighed [testis index = testis weight (mg) ÷ body weight (g)], and processed as follows. Two halves of one testis were snap frozen; one half of the contralateral testis was immersion-fixed in 4% paraformaldehyde overnight at 4 °C, and the other half was fixed in Bouin's solution overnight at room temperature.

2.4 Inductively coupled plasma mass spectrometry (ICP-MS)

Inductively coupled plasma mass spectrometry (ICP-MS) was used to assess silver levels in the testes. Bilateral testes were dissected and washed in PBS, cut in half and halves individually frozen at -80 °C until tissue digestion. Tissues were thawed and transferred to pre-acid-washed and pre-weighed 15 ml perfluoroalkoxy standard vials (Savillex, Eden Prairie, MN) and weighed in vials to determine the wet weight of the tissues. Next, 1 ml of TraceMetal™ grade concentrated nitric acid (Fisher Scientific, Pittsburgh, PA) was added to the vials, sealed tight, and allowed to digest overnight at room temperature. Controls consisted of blanks, blanks with AgNPs spiked at 60 and 600 ppb, and testis halves from control treated mice, also spiked at 60 and 600 ppb. Following digestion, 10 ml of 2% nitric acid was added to the digested samples, and the entire contents decanted into trace metal-free 15 ml polypropylene conical tubes (Corning Inc., Corning, NY). Samples were

centrifuged at 4,000 × g for 15 minutes to pellet any insoluble debris, and 10 ml of supernatant was collected, filtered with a 0.22 μm polyethersulfone syringe filter (EMD Millipore, Billerica, MA), transferred to trace metal-free 50 ml polypropylene conical tubes (Corning Inc), and diluted to a final concentration of 2% HNO3 with the addition of 30 ml Type I water.

Any control or sample known to contain silver nanomaterial was subjected to inductively coupled plasma optical emission spectrometry (ICP-OES) using an Agilent 725 ICP-OES System (Agilent Technologies, Santa Clara, CA) to ensure proper dilutions for subsequent inductively coupled plasma mass spectrometry (ICP-MS) analysis using a Varian 810 ICP-MS System (Agilent Technologies). A series of calibration standards (1 ppb, 10 ppb and 100 ppb) were prepared from the single element standards from Inorganic Ventures (Christiansburg, VA) to construct a calibration line for the off-line data reduction. The sensitivity drift was monitored and corrected through a multiple analysis of a known concentration drift control solution in a matrix matching that of the actual samples. Analytical precision was better than 5% as monitored by the repeated analysis of standard solutions. ICP-OES and ICP-MS measurements were carried out by the Department of Earth and Atmospheric Sciences at the University of Houston.

2.5. Testis stereology

Fixed testis samples were dehydrated in an ethanol series and embedded in paraffin. Six-μm sections of testis were stained with hematoxylin–eosin for histological observation. The volume densities of the testicular tissue components were determined from images taken from a Olympus BX-60 light microscope (Center Valley, PA, US), using the software ImageJ (National Institute of Health, Bethesda, MA, US). For this purpose, a 540-intersection grid was placed on the obtained images of the testis structures being evaluated [29, 30]. Fifteen randomly chosen fields were scored per testis for each animal at 400× magnification. Points were classified as one of the following: apoptotic germ cells, lumen diameter, and epithelial thickness. The seminiferous tubule diameter was measured at 200× magnification using an ocular micrometer calibrated with a stage micrometer. Thirty round or nearly round tubule profiles were chosen randomly and measured for each animal.

2.6. Leydig cell counts and numbers

Individual Leydig cell volumes were obtained from nucleus volumes and the ratios of nucleus to cytoplasm. As the Leydig cell nucleus in the mouse is spherical by light microscopy, the mean nucleus volume was calculated from the mean nucleus diameter. For this purpose, 30 nuclei with evident nucleoli were measured for each animal. Leydig cell nucleus volume was expressed in μm^3 and obtained from the formula $4/3\pi R^3$, in which R = nuclear diameter/2. To calculate the ratio of nucleus to cytoplasm, a 540-point square lattice was placed over the obtained images at 400× magnification, and at least 1000 points over Leydig cells were counted for each animal. The total number of Leydig cells per testis was estimated from the individual Leydig cell volume and from the volume occupied by Leydig cells in the testis parenchyma.

2.7. Computer-Assisted sperm analysis

During isolation, each right cauda epididymis was rinsed and excised in phosphate buffered saline then minced in a 35-mm Petri dish containing 1.0 ml swimout/capacitation medium consisting of Medium HS [31] (in mM: 135 NaCl, 5 KCl, 2 CaCl2, 1 MgSO4, 20 HEPES, 5 glucose, 10 lactic acid, 1 pyruvic acid, pH 7.4) supplemented with 15 mM $NaHCO_3$ and 5 mg bovine serum albumin (BSA) (Fraction V)/ml preheated to 37 °C. The sperm-media suspension was incubated at 37 °C for 10 minutes. The dish was then swirled to obtain a homogenous solution, and a 5-µl aliquot was transferred to 45 µl of supplemented swimout/capacitation medium, which was preheated to 37 °C. After gently pipetting the suspension up and down, a 15-µl aliquot of diluted sperm-media suspension was transferred to one compartment of a preheated 80-µm 2X-CEL Chamber (Hamilton-Thorne Research, Inc., Beverly, MA, US) for computer-assisted sperm analysis using the integrated visual optical system (IVOS) motility analyzer (Hamilton-Thorne Research, Inc., Beverly, MA, US). The operational settings of the IVOS were the standard mouse parameters recommended by the manufacturer. Ten arbitrary and independent fields were captured per animal for analysis.

2.8. Mating assay

On day 12 post-initial dose administration, the control and treated males randomly selected for breeding were housed individually to establish scents to their cages. On days 15, 60, and 120 two untreated female mice were introduced per male's cage and housed for 7 days before the male was removed and housed separately. On day 17 post-initial mating, the females were sacrificed and the pregnancy status and number of fetuses per pregnant female were determined.

2.9. Endocrinology

Serum luteinizing hormone (LH), follicle-stimulating hormone (FSH), and testosterone levels as well as intratesticular testosterone levels from testis homogenates were measured by the University of Virginia Center for Research in Reproduction Ligand Assay and Analysis Core. Luteinizing hormone was measured by a sensitive two-site sandwich immunoassay using monoclonal antibodies against both bovine LH (no. 581B7) and the human LH-beta subunit (no. 5303: Medix Biochemica, Kauniainen, Finland), as previously described [32]. Follicle-stimulating hormone was assayed by radioimmunoassay (RIA) using reagents provided by Dr. A. F. Parlow and the National Hormone and Peptide Program, as previously described [33]. Total testosterone was measured with the Coat-A-Count total testosterone solid phase RIA kit (Siemens Medical Solutions Diagnostics, Los Angeles, CA, US). The LH, FSH, and testosterone assays have sensitivities of 0.07, 2, and 0.1 ng/ml, respectively.

Mouse IGF1 was analyzed at the Endocrine Technology and Support Core Laboratory, Oregon National Primate Research Center, Oregon Health & Sciences University (Beaverton, OR) using the mouse/rat specific IGF1 ILISA kit (Cat. # DG-100, R&D Systems, Minneapolis, MN 55413). The assay has a sensitivity and range of 31.2 - 2000 pg/ml. The inter- and intra-assay variation was 6.7% and 3.6%, respectively.

2.10. Steroidogenic mRNA in testis

RNA was extracted from whole testes by first homogenizing each tissue with a Tissue-Tearor (Biospec Products, Bartlesville, OK), passing individual homogenates through QIAshredder columns (Qiagen, Valencia, CA, US), and finally processing each sample using the RNeasy Mini Kit (Qiagen) according to manufacturer's instructions. Reverse transcription was performed using the SuperScript III Reverse Transcriptase (Invitrogen, Carlsbad, CA, US), and real-time polymerase chain reaction (RT-PCR) was performed using the TaqMan Universal PCR Master Mix (Applied Biosystems, Carlsbad, CA, US), all according to manufacturers' instructions. The expression value of each gene was normalized to the amount of an internal control gene (*Eif3l* or *Rps3*) cDNA in order to calculate the relative amount of RNA in each sample. The expression value of each gene in control was arbitrarily defined as 1 unit. RT-PCR assays were carried out in triplicate and the normalized expression values for all technical repeats were averaged before analysis of the individual samples. A relative quantitative fold change was determined using the ΔΔCt method. Applied Biosystems Taqman Gene Expression Assays used for specific transcripts were: Mm00490735_m1 (*Cyp11a1*), Mm00484040_m1 (*Cyp17a1*), Mm00484049_m1 (*Cyp19a1*), Mm00460859_m1 (*Eif3l*), , Mm00439093_m1 (*Ghr*), Mm01282499_m1 (*Hmgcr*), Mm01304569_m1 (*Hmgcs1*), Mm00515131_m1 (*Hsd17b3*), Mm01261921_mH (*Hsd3b1*), Mm00439560_m1 (*Igf1*), Mm00656272_m1 (*Rps3*), Mm00441558_m1 (*Star*), and Mm00437828_m1 (*Tspo*).

2.11. Statistical analysis

All data were analyzed using GraphPad Prism 6 (GraphPad Software, Inc., La Jolla, CA, US) and are presented as mean ± SEM (standard error of the mean). Comparisons between control and treated groups at one time point were conducted using two-tailed Student's *t*-test; comparisons between control and treated groups at two or more time points were conducted using analysis of variance (ANOVA) followed by Newman–Keuls post-hoc test. For all comparisons, statistical significance was assigned at $P<0.05$.

3. Results

3.1. Characterization of the nanoparticle suspension

The silver concentration of aliquots of AgNP suspension were verified through ICP-OES and ICP-MS and found to be higher than—but within 10%—of the concentration, 1 mg/ml, listed on the product specification sheet (1.07 ± 0.014 mg/ml, mean ± SEM, $n=4$). Additionally, DLS and TEM were used to verify the size, morphology, and dispersion of the nanoparticles once diluted in PBS. The mean diameter of diluted AgNPs was 14 nm as measured through DLS (Fig. 1A), which is higher than the mean (± SD) diameter of 8.6 ± 1.7 nm listed on the specification sheet. Our TEM imaging of nanoparticles dried on the surface of a TEM grid confirmed the presence of monodisperse particles with a mean diameter of 10.4 ± 1.9 nm (mean ± SD; Fig. 1B).

3.2. AgNPs do not affect body and testis weights

Mice were dosed 5 times, once every 3 days over a 12 day period with a total of 0 (control) or 1 (treated) mg/ml AgNP administered per dose (Fig. 2). Animals were observed each day

during treatment to ensure good health. All mice in the treated group appeared to be in good health and behaved no differently from controls. To further determine the general toxicity of AgNPs, body and testis weights of the mice were measured. There were no significant differences in body weight between the treated and control groups at 3, 6, 9, 12, 15, 30, 60, 90, and 120 days post-initial exposure (Fig. 3A). Additionally, no statistically significant differences ($P>0.05$) in the mean testis weights and mean testis indices (testis weight [mg] / body weight [g]) were found for animals at 15, 60, and 120 days post-initial exposure (Fig. 3B, C).

3.3. High levels of silver are present in the testes of treated mice

To determine whether AgNPs reached the testes after 12 days of treatment we measured elemental silver levels in the testes of control and treated mice at 15 days post-initial treatment. As shown in Figure 4, the mean (± SEM) value of Ag^{107} and Ag^{109} in control mice ($n=3$) was very low at 6.03 ± 4.09 and 5.71 ± 4.08 pg/g testis, respectively. Treated mice on the other hand showed a statistically significant ($P<0.0001$) increase in Ag^{107} and Ag^{109} levels at 2.69 ± 0.13 and 2.65 ± 0.12 ng/g testis, respectively (Fig. 4). As additional controls, separate testis halves from the same control testes assessed for background Ag levels were spiked with known amounts, 60 and 600 ppb, of AgNP solution prior to acid digestion. Whereas Ag levels from blanks spiked with known quantities of AgNP solution corresponded to within 10% of the listed Ag concentration, Ag levels from spiked, control tissue digests were reduced to ½ to ⅓ of the amount that should have been present, indicating a loss of silver during preparation, most likely due to precipitation with insoluble material, which was removed through centrifugation and filtration. Therefore, the true silver levels in the testes of treated mice were most likely greater.

To determine the persistence of silver in the testes of treated mice, we measured silver levels in the testes of control and treated mice at 120 days post-initial treatment. Just as the treated mice at 15 days post-initial treatment showed significantly elevated levels of silver in the testes when compared to controls, treated mice at 120 days had significantly elevated levels, which was approximately 1/3 the level seen at 15 days: Ag^{107} and Ag^{109} in control mice ($n=3$) was 5.96 ± 0.30 and 5.80 ± 0.27 pg/g testis, respectively, while treated mice ($n=3$) showed significantly ($P<0.005$) elevated Ag^{107} and Ag^{109} levels at 0.90 ± 0.13 and 0.85 ± 0.12 ng/g testis, respectively (Fig. 4).

3.4. AgNP treatment resulted in histopathological alterations of the testes

Although the mean testis weights for controls and treated mice did not differ significantly (Fig. 3), several testis parameters were significantly altered in treated mice. Lumen volume and tubule diameter were significantly increased ($P<0.05$) and seminiferous epithelium volume density was significantly decreased ($P<0.05$) in the treated animals at 15 and 60 days post-initial exposure, although these parameters returned to levels not significantly different from controls at 120 days (Fig. 5, 6A-C). Similarly, the percentage of apoptotic germ cells was significantly increased ($P<0.05$) in treated animals at 15, 60, and 120 days, although the number of apoptotic germ cells at 120 days was reduced relative to 15 and 60 days (Fig. 5, 6D).

3.5. AgNP treatment does not alter overall sperm fitness or fertility

Despite these significant histomorphometric findings, no significant differences ($P>0.05$) between control and treated male mice at 15, 60, and 120 days were found relating to cauda epididymal sperm concentration or sperm motility parameters. However, several sperm motility parameters at day 60 neared significance with *P*-values between 0.05 and 0.1. Smoothed path velocity (VAP), straight line velocity (VSL), track velocity (VCL), amplitude of lateral head displacement (ALH), and straightness (STR; VSL/VAP) had *P*-values of 0.066, 0.056, 0.060, 0.074 and 0.078, respectively (Table I). Consistently, treated males housed with two females each for 7 days at 15, 60, and 120 days post-initial treatment all sired fetuses of similar numbers (Table II).

3.6. Serum and intratesticular testosterone levels are significantly elevated in treated mice

Next, we determined the serum levels of LH, FSH, and testosterone in controls and AgNP-treated mice at 15, 60, and 120 days post-initial exposure. Figure 7 shows that although AgNP treatment did not alter the serum levels of LH and FSH at 15, 60, and 120 days post-initial exposure, it did significantly increase serum testosterone levels at 15 days post-initial exposure ($P<0.05$). At 60 and 120 days post-initial treatment, however—although an increase in testosterone was still present in the treated animals compared to controls—the differences were not statistically significant ($P>0.05$) (Fig. 7C).

To determine whether the increase in serum testosterone was due to increased production of testosterone in the testes, we next determined the intratesticular levels of testosterone in control and treated animals at 15 and 120 days post-initial treatment. Testis homogenates of control and treated animals at 15 days post-initial treatment were similarly measured for testosterone levels, revealing a significant ($P<0.05$) increase in intratesticular testosterone concentration in the treated animals (Fig. 7D). However, at 120 days post-initial treatment, intratesticular testosterone levels were not significantly different ($P>0.05$) between control and treated groups (Fig. 7D).

Lastly, since IGF1 can regulate the expression of enzymes involved the synthesis of testosterone [34, 35], we determined the levels of serum IGF1 in treated and control mice at 15 days post-initial treatment. As seen in Figure 7E, serum IGF1 levels were not significantly different ($P>0.05$) in treated mice as compared to controls.

3.7. An increase in testosterone is correlated with an increase in Leydig cell size

The Leydig cell volume density (Fig. 8A) and numbers of Leydig cells per testis and per gram of testis (Fig. 8B) remained similar ($P>0.05$) among the control and treated groups at 15, 60, and 120 days post-initial exposure; however, both the cytoplasm and overall size of Leydig cells were significantly increased ($P<0.05$) in the treated groups at all time points (Fig. 8D, E). Interestingly, although Leydig cell nuclear volume was significantly increased in size ($P<0.05$) at 15 and 60 days, this parameter returned to a level not significantly different from controls at 120 days (Fig. 8).

3.8. Steroidogenic mRNA in testis

Since increases in serum and intratesticular testosterone suggested that Leydig cell production of testosterone was upregulated, we next examined the transcription levels of enzymes involved in cholesterol, testosterone, and estradiol biosynthesis using fragments of whole testes.

Testosterone is derived from cholesterol, which is synthesized from Acetyl-CoA through a process that needs the enzymes 3-hydroxy-3-methylglutaryl-CoA reductase (HMGCR) and 3-hydroxy-3-methylglutaryl-CoA synthase 1 (HMGCS1) [36]. In Leydig cells, cholesterol destined to steroidogenesis is transported from the outer to the inner mitochondrial membrane through transporters such as steroidogenic acute regulatory protein (StAR) [37] and translocator protein (TSPO) [38]. Transcript levels of *Hmgcr*, *Hmgcs1*, *Star*, and *Tspo*, were not significantly different from those of controls (Fig. 9A, B).

The *Cyp11a1* gene encodes the cholesterol side-chain cleavage enzyme (P450scc) that catalyzes the first step for the biosynthesis of sex hormones, including testosterone [39]. We found a significant increase in *Cyp11a1* levels in the testes of treated animals (Fig. 9C). Additionally, transcripts for *Hsd3b1*, a gene encoding another enzyme in the steroid biosynthesis pathway, were significantly increased compared with controls (Fig. 9C); however, transcripts for the genes encoding the enzymes *Cyp17a1*, *Hsd17b3*, *and Cyp19a1* were not significantly different between controls and treated mice (Fig. 9C).

Because *Cyp11a1* expression is regulated by growth hormone and insulin-like growth factor 1 (IGF1) signaling [34, 35], we measured mRNAs of *Ghr* and *Igf1* in the testis. Expression of *Igf1* was increased in the testes of AgNP-treated animals but not in a significant manner (Fig. 9D). Similarly, expression of the growth hormone receptor was visibly increased, but the difference with the control was not statistically significant ($P>0.05$) (Fig. 9D).

4. Discussion

Considering the plethora and rise of consumer products containing AgNPs, the likelihood of human exposure warrants male reproductive toxicity assessment. However, the concentration of AgNPs released from consumer products or present in workplace air are not known. Similarly, data on the concentrations of AgNPs in human tissues, including the testes, due to inhalation, oral, or dermal exposure are incomplete. Previous studies from our lab examining the *in vitro* effect of AgNPs on C18-4, a spermatogonial stem cell line, found acute effects that if recapitulated *in vivo* would be deleterious to male fertility [22, 23]. In the present study, we examined the *in vivo* effect of AgNPs on the testes and male germ line. Because the concentrations that were tested *in vitro* were above presumptive exposure and only germ cells were tested, we injected AgNPs into the tail vein to obtain bioequivalent serum concentrations. Testes weights, sperm cell numbers, and male fertility were unaffected in our study. The *in vivo* data obtained in the present study thus provide evidence that sub-acute injection of AgNPs can cause histomorphometric changes in the germ cell compartment including subtle, but significant increases in germ cell apoptosis, but our data indicates that AgNPs do not affect spermatogonial stem cells directly.

We chose intravenous administration for NP delivery over oral, dermal, and inhalation means of administration because injection bypasses absorption and allows for other aspects of toxicokinetic processes, such as tissue distribution and elimination, to be studied with precision. The time points of 15, 60, and 120 days post-initial administration were chosen to examine the various potential immediate and long-term consequences of AgNP exposure. We anticipated finding changes in sperm concentration or motility, mating behavior, or the pregnancy rate at 15 days post-initial administration if the AgNPs had had immediate and detrimental effects on mating behavior, or sperm maturation; however, we observed no adverse effects at this time point other than significant effects on testis histomorphometry and significant increases in serum and intratesticular testosterone. At 60 days post-initial administration, testicular atrophy and decreases in both sperm production and overall fertility would have been evident if AgNPs had had a detrimental impact on spermatogonial stem cell maintenance, proliferation, and/or differentiation, as has been demonstrated before in instances of chemotoxic insult [40, 41]. However, no such effects were observed. Given that detrimental effects were observed in our previous *in vitro* studies, our current results suggest that stem cells *in vivo* do not receive equivalent amounts of NP exposure despite similar bioavailability. Finally, if detrimental effects had been observed at 15 or 60 days post-initial exposure, the capacity of the testes to recover under the present conditions would have been revealed at 120 days [40, 41]. As only small, but significant effects were observed at 15 or 60 days, it is unsurprising that we found no effects on any histology or fertility parameters at 120 days.

With the exception of one high dose administration study of AgNPs (30, 125, and 500 mg/kg orally for 90 days) that demonstrated a dose-dependent decrease in body weight [19], all other studies have indicated that exposure to AgNPs does not significantly alter body weight. The doses studied varied from 1 mg/kg orally every day for 14 days to a single dose of 0.5 and 5 mg/kg intravenously to 49, 133, and 515 $\mu g/m^3$ inhalation for 90 days [20, 21, 42, 43]. Studies investigating other types of nanoparticles did not demonstrate any changes of body weight either. For example, carbon nanotubes were intravenously administered using 5 doses over 12 days at 5mg/kg per dose [25], carbon black nanoparticles were instilled intratracheally at a dose of 0.1 mg/mouse once a week for 10 weeks [5, 25, 28] and silica-coated magnetic nanoparticles were intraperitoneally administered at doses of 25, 50, and 100 mg/kg for 4 weeks [19]. Our finding that body weights were not significantly altered throughout the treatment protocol with much lower AgNPs concentrations is consistent with these studies.

As is the case with body weight, all studies except for one [19] have found that exposure to AgNPs [20, 21, 42, 43] or NPs comprised of carbon or nanoparticle-rich diesel exhaust (NRDE) [25, 27, 28] does not significantly alter testis weight. Our finding that testis weights were not significantly altered at 15, 60, and 120 days is thus consistent with the majority of previous findings. Considering testis weight and size are highly correlated with proper germ cell maintenance, proliferation, and differentiation, this finding in itself indicates that sub-acute administration of AgNPs does not directly interfere with spermatogenesis. However, potential downstream effects, such as those on sperm maturation and function, mating

behavior, and ultimately, fertility, cannot be ascertained through the measurement of testis weight alone, and need to be gauged through additional testing of the kind in this report.

Recent studies in rabbits and rats intravenously injected with a single dose (5 mg/kg) of AgNPs and assessed histologically 1, 7, and 28 days post-exposure, found DNA damage and degeneration of germ cells in the testes of treated animals [21, 43]. NRDE [27] and nanomaterials such as carbon-black NPs [28] and carbon nanotubes [25] have also been found to have significant effects on testis histology in rodents. Mice intratracheally administered with a single weekly dose of carbon-black NPs for 10 weeks showed partial vacuolation of the seminiferous tubules and elevated serum testosterone levels [28]. Bai and colleagues demonstrated that multiwalled carbon nanotubes intravenously administered into male mice decreased the height of the seminiferous epithelium in testes at 15-days post-initial exposure, but the damage was repaired by 60- and 90-days [25]. Interestingly, the authors found that fertility and the pregnancy rates of the animals were unaffected, demonstrating that this reversible testis damage had negligible effects on overall testicular function and that the histological effect of nanotubes on the weight of the testes is negligible. Finally, the study of Li and colleagues, which examined the effects of NRDE found that seminiferous tubules in NRDE-exposed animals displayed degeneration and necrosis with desquamation of the seminiferous epithelium and loss of spermatozoa as well as interstitial edema [27]. Our findings that intravenous injection of mice with AgNPs causes a decrease in seminiferous epithelium height, an increase in lumen volume, and an increase in apoptotic germ cells are consistent with the data described by these studies.

Proper levels of LH, FSH, and testosterone are critical for spermatogenesis; however, environmental toxicants or endocrine disruptors such as phthalates and polychlorinated biphenyls can disrupt the production and regulation of these hormones [2, 44]. These disruptions result in testicular injury, malfunction in spermatogenesis, and male infertility [45-48]. Carbon-black NPs [28] and NRDE [27] have both been found to significantly increase testosterone levels in exposed male rodents. An interesting and unexpected finding of our investigation was that serum and intratesticular testosterone were also significantly elevated in response to AgNP exposure. Significant increases in Leydig cell size and expression of *Cyp11a1* and *Hsdb31* mRNA were consistent with this finding. Leydig cell hypertrophy is associated with increased steroid biosynthesis [49]. Increases in *Cyp11a1* and *Hsd3b1*, two enzymes involved in the steroid biosynthetic pathway, are consistent with increases in serum and intratesticular testosterone. Similarly, Ramdhan et al. also found increased *Cyp11a1* mRNA expression in the testes of NRDE-exposed animals [50].

In the testis, cholesterol import to the inner mitochondrial membrane of Leydig cells is the rate-limiting step in testosterone biosynthesis. This mechanism relies on the formation of a protein complex that assembles at the outer mitochondrial membrane called the transduceosome [51]. The transduceosome consists of several cytosolic and mitochondrial proteins, including steroidogenic acute regulatory protein (StAR) [37], which brings cholesterol to the mitochondria from cytosolic stores. In the present study, we could not demonstrate a significant increase in *Star* expression in the presence of AgNPs; however, after translocation to the inner mitochondrial membrane, which is mediated by TSPO, cholesterol interacts with the CYP11A1 side chain cleavage enzyme to be converted to

pregnenolone and eventually testosterone through several enzymatic steps involving the enzyme HSD3B1. Given that we found increases in *Cyp11a1* and *Hsd3b1*, which were consistent with the increase in testosterone, but did not find increases in *Star* levels, one possibility is that post-translational modifications important in regulating StAR activity (reviewed in [52]), such as through phosphorylation [53], were altered.

CYP11A1 production is, at least in part, regulated by growth hormone (GH) and IGF1 [34, 35]. Increases in intratesticular testosterone and *Cyp11a1* expression have previously been shown to coincide with increases in *Ghr* and *Igf1* expression in the testes of NRDE-exposed mice [50]. In the present study, however, we could not detect significant increases in *Ghr* or *Igf1* produced by the testicular somatic cells. That being said, it is well known that after inhalation or ingestion, NPs accumulate preferentially in the liver [5, 8, 19], and thus, increased *Cyp11a1* expression in the Leydig cells might be caused by systemic increases in IGF1 production by the liver; however, in our study serum IGF1 levels were not significantly increased (Fig. 7E), just as LH and FSH were not significantly different (Fig. 7A, B). It is possible we observed an increase in testosterone without a corresponding decrease in LH, since LH levels fluctuate widely with an inherent cyclicity [54], thus necessitating a considerably larger sample size to discern a difference.

Recent data from Loeschner et al. (2011) demonstrates that the organ distribution of silver was similar regardless of whether AgNPs or silver acetate was administered orally to rats, indicating tissue distribution of silver in AgNP administered animals arose from rapid free ion release [55, 56]. Indeed, shortly after intravenous injection, free silver ions may have been released from the nanoparticles administered in our test animals. Although we were able to demonstrate the presence of high levels of silver in the testes of treated mice, this information alone does not prove the presence of silver nanoparticles. Therefore, we cannot make the determination of whether the biological effects observed in this study were due to particle-specific effects or the distant or local release of silver ions from the nanoparticles. However, our previous *in vitro* studies demonstrated that the levels of free ions, if any, were insufficient to confer the toxic effects observed on cultured cells. In one experiment where silver carbonate was added directly to the culture medium [57], or another where medium pre-treated with nanoparticles and removed through centrifugation was then added to the cells [23], neither of these treatments conferred effects significantly different from controls [23, 57]. Additionally, previous studies showing similar testosterone increases in nanoparticle rich diesel exhaust (NRDE) exposed rodents [27, 50] support the possibility that the effects observed in our study are particle, and not free ion specific.

5. Conclusion

In summary, the present study demonstrates potential adverse effects on the male reproductive function of mice following sub-acute AgNP exposure, and to the best of our knowledge, is the first to report that AgNP exposure can lead to Leydig cell alterations and increases in intratesticular testosterone. Because testosterone can inhibit spermatogonial differentiation independently of GnRH [58], our study underscores the possibility that chronic AgNP exposure might ultimately have a negative impact on male fertility.

Acknowledgments

This work was supported by NIH HD044543 and HD054607 to MCH, NIH T32 ES007326 fellowship to TG, and in part through Cancer Center Support Grant CA16672. We are also grateful to Lou Ann Miller with the Frederick Seitz Materials Research Laboratory Central Facilities at the University of Illinois at Urbana-Champaign for sample preparation for—and analysis with—TEM; Dr. Cristian Rodriguez-Aguayo at The University of Texas MD Anderson Cancer Center for assistance in measuring particle size distribution through DLS; Dr. Parmeswaran Diagaradjane at The University of Texas MD Anderson Cancer Center for his valuable input regarding tissue preparation for ICP-MS; Dr. Yongjun Gao and Minako Righter at the University of Houston Department of Earth and Atmospheric Sciences for performing ICP- OES and ICP-MS analyses; and Dr. Francis Pau and the Endocrine Technology and Support Core Laboratory at Oregon National Primate Research Center, Oregon Health & Sciences University for analyzing mouse IGF1 for this study. LH, FSH, and testosterone assays performed at University of Virginia Center for Research in Reproduction Ligand Assay and Analysis Core were supported by National Institute of Child Health and Human Development (NICHD) Specialized Cooperative Centers Program in Reproduction Research grant U54-HD28934 to the University of Virginia Center for Research in Reproduction Ligand Assay and Analysis Core, which is also supported by the Eunice Kennedy Shriver NICHD/NIH (SCCPIR) Grant U54-HD28934.

References

1. Pryor JL, Hughes C, Foster W, Hales BF, Robaire B. Critical windows of exposure for children's health: the reproductive system in animals and humans. Environ Health Perspect. 2000; 108(Suppl 3):491–503. [PubMed: 10852849]
2. Lucas B, Fields C, Hofmann MC. Signaling pathways in spermatogonial stem cells and their disruption by toxicants. Birth Defects Res C Embryo Today. 2009; 87:35–42. [PubMed: 19306349]
3. Lucas BE, Fields C, Joshi N, Hofmann MC. Mono-(2-ethylhexyl)-phthalate (MEHP) affects ERK-dependent GDNF signalling in mouse stem-progenitor spermatogonia. Toxicology. 2012; 299:10–9. [PubMed: 22564763]
4. Kashiwada S. Distribution of nanoparticles in the see-through medaka (Oryzias latipes). Environ Health Perspect. 2006; 114:1697–702. [PubMed: 17107855]
5. Kim JS, Yoon TJ, Yu KN, Kim BG, Park SJ, Kim HW, et al. Toxicity and tissue distribution of magnetic nanoparticles in mice. Toxicol Sci. 2006; 89:338–47. [PubMed: 16237191]
6. Oberdorster G. Safety assessment for nanotechnology and nanomedicine: concepts of nanotoxicology. J Intern Med. 2010; 267:89–105. [PubMed: 20059646]
7. De Jong WH, Borm PJ. Drug delivery and nanoparticles:applications and hazards. Int J Nanomedicine. 2008; 3:133–49. [PubMed: 18686775]
8. Kwon JT, Hwang SK, Jin H, Kim DS, Minai-Tehrani A, Yoon HJ, et al. Body distribution of inhaled fluorescent magnetic nanoparticles in the mice. J Occup Health. 2008; 50:1–6. [PubMed: 18285638]
9. Sharma HS, Hussain S, Schlager J, Ali SF, Sharma A. Influence of nanoparticles on blood-brain barrier permeability and brain edema formation in rats. Acta Neurochir Suppl. 2010; 106:359–64. [PubMed: 19812977]
10. Jain J, Arora S, Rajwade JM, Omray P, Khandelwal S, Paknikar KM. Silver nanoparticles in therapeutics: development of an antimicrobial gel formulation for topical use. Mol Pharm. 2009; 6:1388–401. [PubMed: 19473014]
11. Park EJ, Yi J, Kim Y, Choi K, Park K. Silver nanoparticles induce cytotoxicity by a Trojan-horse type mechanism. Toxicol In Vitro. 2010; 24:872–8. [PubMed: 19969064]
12. Ahamed M, Karns M, Goodson M, Rowe J, Hussain SM, Schlager JJ, et al. DNA damage response to different surface chemistry of silver nanoparticles in mammalian cells. Toxicol Appl Pharmacol. 2008; 233:404–10. [PubMed: 18930072]
13. Carlson C, Hussain SM, Schrand AM, Braydich-Stolle LK, Hess KL, Jones RL, et al. Unique cellular interaction of silver nanoparticles: size-dependent generation of reactive oxygen species. J Phys Chem B. 2008; 112:13608–19. [PubMed: 18831567]
14. Ahamed M, Posgai R, Gorey TJ, Nielsen M, Hussain SM, Rowe JJ. Silver nanoparticles induced heat shock protein 70, oxidative stress and apoptosis in Drosophila melanogaster. Toxicol Appl Pharmacol. 2010; 242:263–9. [PubMed: 19874832]

15. Asharani PV, Hande MP, Valiyaveettil S. Anti-proliferative activity of silver nanoparticles. BMC Cell Biol. 2009; 10:65. [PubMed: 19761582]
16. Asharani PV, Low Kah Mun G, Hande MP, Valiyaveettil S. Cytotoxicity and genotoxicity of silver nanoparticles in human cells. ACS Nano. 2009; 3:279–90. [PubMed: 19236062]
17. Cha K, Hong HW, Choi YG, Lee MJ, Park JH, Chae HK, et al. Comparison of acute responses of mice livers to short-term exposure to nano-sized or micro-sized silver particles. Biotechnol Lett. 2008; 30:1893–9. [PubMed: 18604478]
18. Sung JH, Ji JH, Yoon JU, Kim DS, Song MY, Jeong J, et al. Lung function changes in Sprague-Dawley rats after prolonged inhalation exposure to silver nanoparticles. Inhal Toxicol. 2008; 20:567–74. [PubMed: 18444009]
19. Kim YS, Song MY, Park JD, Song KS, Ryu HR, Chung YH, et al. Subchronic oral toxicity of silver nanoparticles. Part Fibre Toxicol. 2010; 7:20. [PubMed: 20691052]
20. Park EJ, Bae E, Yi J, Kim Y, Choi K, Lee SH, et al. Repeated-dose toxicity and inflammatory responses in mice by oral administration of silver nanoparticles. Environ Toxicol Pharmacol. 2010; 30:162–8. [PubMed: 21787647]
21. Lee Y, Kim P, Yoon J, Lee B, Choi K, Kil KH, et al. Serum kinetics, distribution and excretion of silver in rabbits following 28 days after a single intravenous injection of silver nanoparticles. Nanotoxicology. 2012 In Press.
22. Braydich-Stolle L, Hussain S, Schlager JJ, Hofmann MC. In vitro cytotoxicity of nanoparticles in mammalian germline stem cells. Toxicological sciences. 2005; 88:412–9. [PubMed: 16014736]
23. Braydich-Stolle LK, Lucas B, Schrand A, Murdock RC, Lee T, Schlager JJ, et al. Silver nanoparticles disrupt GDNF/Fyn kinase signaling in spermatogonial stem cells. Toxicological sciences : an official journal of the Society of Toxicology. 2010; 116:577–89. [PubMed: 20488942]
24. Hofmann MC, Braydich-Stolle L, Dettin L, Johnson E, Dym M. Immortalization of mouse germ line stem cells. Stem Cells. 2005; 23:200–10. [PubMed: 15671143]
25. Bai Y, Zhang Y, Zhang J, Mu Q, Zhang W, Butch ER, et al. Repeated administrations of carbon nanotubes in male mice cause reversible testis damage without affecting fertility. Nat Nanotechnol. 2010; 5:683–9. [PubMed: 20693989]
26. De Jong WH, Hagens WI, Krystek P, Burger MC, Sips AJ, Geertsma RE. Particle size-dependent organ distribution of gold nanoparticles after intravenous administration. Biomaterials. 2008; 29:1912–9. [PubMed: 18242692]
27. Li C, Taneda S, Taya K, Watanabe G, Li X, Fujitani Y, et al. Effects of inhaled nanoparticle-rich diesel exhaust on regulation of testicular function in adult male rats. Inhal Toxicol. 2009; 21:803–11. [PubMed: 19653803]
28. Yoshida S, Hiyoshi K, Ichinose T, Takano H, Oshio S, Sugawara I, et al. Effect of nanoparticles on the male reproductive system of mice. Int J Androl. 2009; 32:337–42. [PubMed: 18217983]
29. Costa GM, Leal MC, Ferreira CS, Guimaraes DA, Franca LR. Duration of spermatogenesis and spermatogenic efficiency in 2 large neotropical rodent species: the agouti (Dasyprocta leporina) and paca (Agouti paca). J Androl. 2010; 31:489–99. [PubMed: 20378926]
30. Rodriguez-Sosa JR, Costa GM, Rathi R, Franca LR, Dobrinski I. Endocrine modulation of the recipient environment affects development of bovine testis tissue ectopically grafted in mice. Reproduction. 2012; 144:37–51. [PubMed: 22550313]
31. Burnett LA, Blais EM, Unadkat JD, Hille B, Tilley SL, Babcock DF. Testicular expression of Adora3i2 in Adora3 knockout mice reveals a role of mouse A3Ri2 and human A3Ri3 adenosine receptors in sperm. J Biol Chem. 2010; 285:33662–70. [PubMed: 20732875]
32. Haavisto AM, Pettersson K, Bergendahl M, Perheentupa A, Roser JF, Huhtaniemi I. A supersensitive immunofluorometric assay for rat luteinizing hormone. Endocrinology. 1993; 132:1687–91. [PubMed: 8462469]
33. Gay VL, Midgley AR Jr, Niswender GD. Patterns of gonadotrophin secretion associated with ovulation. Fed Proc. 1970; 29:1880–7. [PubMed: 5529888]
34. Xu YP, Chedrese PJ, Thacker PA. Growth hormone amplifies insulin-like growth factor I induced progesterone accumulation and P450scc mRNA expression. Mol Cell Endocrinol. 1995; 111:199–206. [PubMed: 7556882]

35. Wang GM, O'Shaughnessy PJ, Chubb C, Robaire B, Hardy MP. Effects of insulin-like growth factor I on steroidogenic enzyme expression levels in mouse leydig cells. Endocrinology. 2003; 144:5058–64. [PubMed: 12959969]
36. Eacker SM, Agrawal N, Qian K, Dichek HL, Gong EY, Lee K, et al. Hormonal regulation of testicular steroid and cholesterol homeostasis. Mol Endocrinol. 2008; 22:623–35. [PubMed: 18032697]
37. Stocco DM, Clark BJ. Role of the steroidogenic acute regulatory protein (StAR) in steroidogenesis. Biochem Pharmacol. 1996; 51:197–205. [PubMed: 8573184]
38. Papadopoulos V, Baraldi M, Guilarte TR, Knudsen TB, Lacapere JJ, Lindemann P, et al. Translocator protein (18kDa): new nomenclature for the peripheral-type benzodiazepine receptor based on its structure and molecular function. Trends Pharmacol Sci. 2006; 27:402–9. [PubMed: 16822554]
39. Payne AH, Hales DB. Overview of steroidogenic enzymes in the pathway from cholesterol to active steroid hormones. Endocr Rev. 2004; 25:947–70. [PubMed: 15583024]
40. Bucci LR, Meistrich ML. Effects of busulfan on murine spermatogenesis: cytotoxicity, sterility, sperm abnormalities, and dominant lethal mutations. Mutat Res. 1987; 176:259–68. [PubMed: 3807936]
41. Zohni K, Zhang X, Tan SL, Chan P, Nagano MC. The efficiency of male fertility restoration is dependent on the recovery kinetics of spermatogonial stem cells after cytotoxic treatment with busulfan in mice. Hum Reprod. 2012; 27:44–53. [PubMed: 22082982]
42. Sung JH, Ji JH, Park JD, Yoon JU, Kim DS, Jeon KS, et al. Subchronic inhalation toxicity of silver nanoparticles. Toxicol Sci. 2009; 108:452–61. [PubMed: 19033393]
43. Gromadzka-Ostrowska J, Dziendzikowska K, Lankoff A, Dobrzynska M, Instanes C, Brunborg G, et al. Silver nanoparticles effects on epididymal sperm in rats. Toxicology letters. 2012
44. Yeung BH, Wan HT, Law AY, Wong CK. Endocrine disrupting chemicals: Multiple effects on testicular signaling and spermatogenesis. Spermatogenesis. 2011; 1:231–9. [PubMed: 22319671]
45. Lehmann KP, Phillips S, Sar M, Foster PM, Gaido KW. Dose-dependent alterations in gene expression and testosterone synthesis in the fetal testes of male rats exposed to di (n-butyl) phthalate. Toxicological sciences : an official journal of the Society of Toxicology. 2004; 81:60–8. [PubMed: 15141095]
46. Naciff JM, Hess KA, Overmann GJ, Torontali SM, Carr GJ, Tiesman JP, et al. Gene expression changes induced in the testis by transplacental exposure to high and low doses of 17{alpha}-ethynyl estradiol, genistein, or bisphenol A. Toxicological sciences : an official journal of the Society of Toxicology. 2005; 86:396–416. [PubMed: 15901920]
47. Ferrara D, Hallmark N, Scott H, Brown R, McKinnell C, Mahood IK, et al. Acute and long-term effects of in utero exposure of rats to di(n-butyl) phthalate on testicular germ cell development and proliferation. Endocrinology. 2006; 147:5352–62. [PubMed: 16916955]
48. Ryu JY, Lee BM, Kacew S, Kim HS. Identification of differentially expressed genes in the testis of Sprague-Dawley rats treated with di(n-butyl) phthalate. Toxicology. 2007; 234:103–12. [PubMed: 17379376]
49. Heller CG, Leach DR. Quantification of Leydig cells and measurement of Leydig-cell size following administration of human chorionic gonadotrophin to normal men. Journal of reproduction and fertility. 1971; 25:185–92. [PubMed: 5558380]
50. Ramdhan DH, Ito Y, Yanagiba Y, Yamagishi N, Hayashi Y, Li C, et al. Nanoparticle-rich diesel exhaust may disrupt testosterone biosynthesis and metabolism via growth hormone. Toxicol Lett. 2009; 191:103–8. [PubMed: 19699283]
51. Midzak A, Rone M, Aghazadeh Y, Culty M, Papadopoulos V. Mitochondrial protein import and the genesis of steroidogenic mitochondria. Mol Cell Endocrinol. 2011; 336:70–9. [PubMed: 21147195]
52. Manna PR, Dyson MT, Stocco DM. Regulation of the steroidogenic acute regulatory protein gene expression: present and future perspectives. Mol Hum Reprod. 2009; 15:321–33. [PubMed: 19321517]

53. Arakane F, King SR, Du Y, Kallen CB, Walsh LP, Watari H, et al. Phosphorylation of steroidogenic acute regulatory protein (StAR) modulates its steroidogenic activity. J Biol Chem. 1997; 272:32656–62. [PubMed: 9405483]

54. Shaw ND, Butler JP, McKinney SM, Nelson SA, Ellenbogen JM, Hall JE. Insights into puberty: the relationship between sleep stages and pulsatile LH secretion. The Journal of clinical endocrinology and metabolism. 2012; 97:E2055–62. [PubMed: 22948756]

55. Loeschner K, Hadrup N, Qvortrup K, Larsen A, Gao X, Vogel U, et al. Distribution of silver in rats following 28 days of repeated oral exposure to silver nanoparticles or silver acetate. Part Fibre Toxicol. 2011; 8:18. [PubMed: 21631937]

56. Xiu ZM, Zhang QB, Puppala HL, Colvin VL, Alvarez PJ. Negligible particle-specific antibacterial activity of silver nanoparticles. Nano Lett. 2012; 12:4271–5. [PubMed: 22765771]

57. Braydich-Stolle L, Hussain S, Schlager JJ, Hofmann MC. In vitro cytotoxicity of nanoparticles in mammalian germline stem cells. Toxicological sciences : an official journal of the Society of Toxicology. 2005; 88:412–9. [PubMed: 16014736]

58. Shetty G, Weng CC, Meachem SJ, Bolden-Tiller OU, Zhang Z, Pakarinen P, et al. Both testosterone and follicle-stimulating hormone independently inhibit spermatogonial differentiation in irradiated rats. Endocrinology. 2006; 147:472–82. [PubMed: 16210366]

Highlights

- Silver nanoparticles were intravenously injected into male *CD1* mice over 12 days.
- Sperm concentration and motility, and mating and fertility indices were normal.
- Leydig cell function was altered, resulting in increased testosterone levels.
- *Cyp11a1* and *Hsd3b1* intratesticular mRNA was increased in treated mice.
- Silver nanoparticles are potentially toxic to male reproduction.

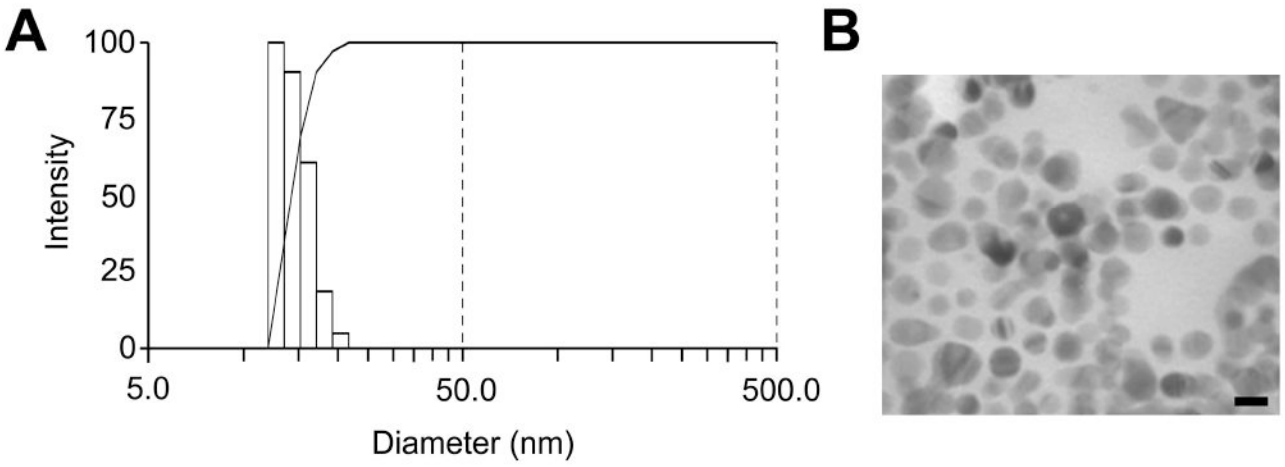

Figure 1.

Size characterization of the silver nanoparticle suspension. Size distribution (Panel A) as determined by dynamic light scattering and transmission electron micrograph (Panel B) of the silver nanoparticles once diluted in PBS. Scale bar equals 10 nm.

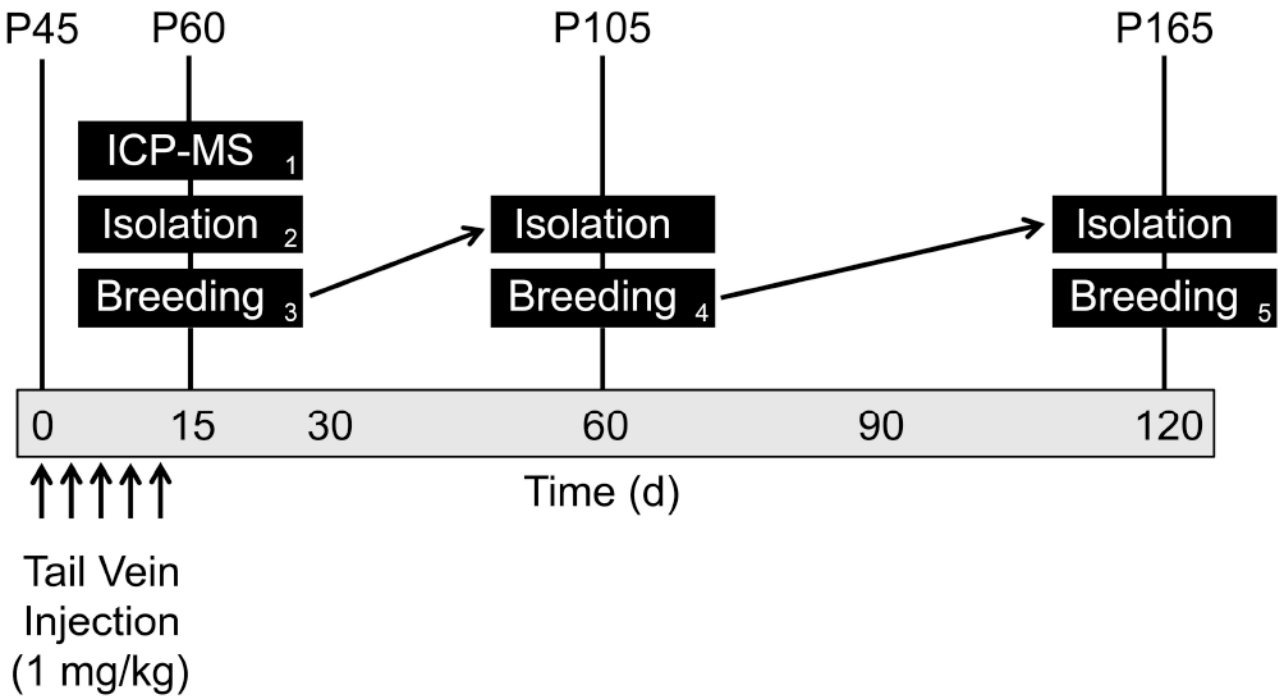

Figure 2.

Overview of the study design. Beginning at approximately postnatal day 45 (P45), mice were administered 1 mg/kg AgNPs through tail vein injection 5 times, once every 3 days (corresponding to days 0, 3, 6, 9, and 12 post-exposure). Per post-exposure time point assessed (15, 60, and 120 days post-initial exposure), six control and six treated mice were used for isolation of blood, testes, and sperm. Meanwhile, a separate group of six control and six treated mice were used for breeding assessment. The numbers on the bottom right corner of the black boxes indicate a group of mice.

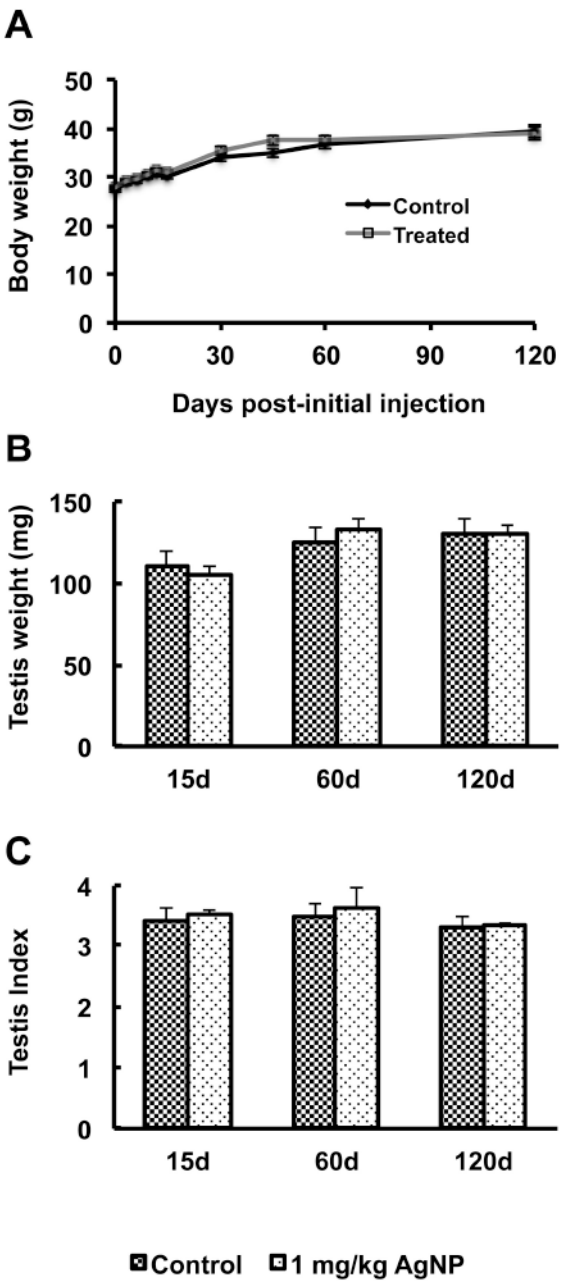

Figure 3.

Body and testis weights after AgNP treatment. Body weights (Panel A), testis weights (Panel B), and testis indices (Panel C; testis weight [mg] / body weight [g]) were measured at the indicated time points after initial exposure. No statistically significant differences were found at any time point. Each measurement is presented as mean ± the standard error of the mean (SEM). Body weights were analyzed by ANOVA with days of weighing as repeated measure. Testes weights were analyzed by two-way ANOVA.

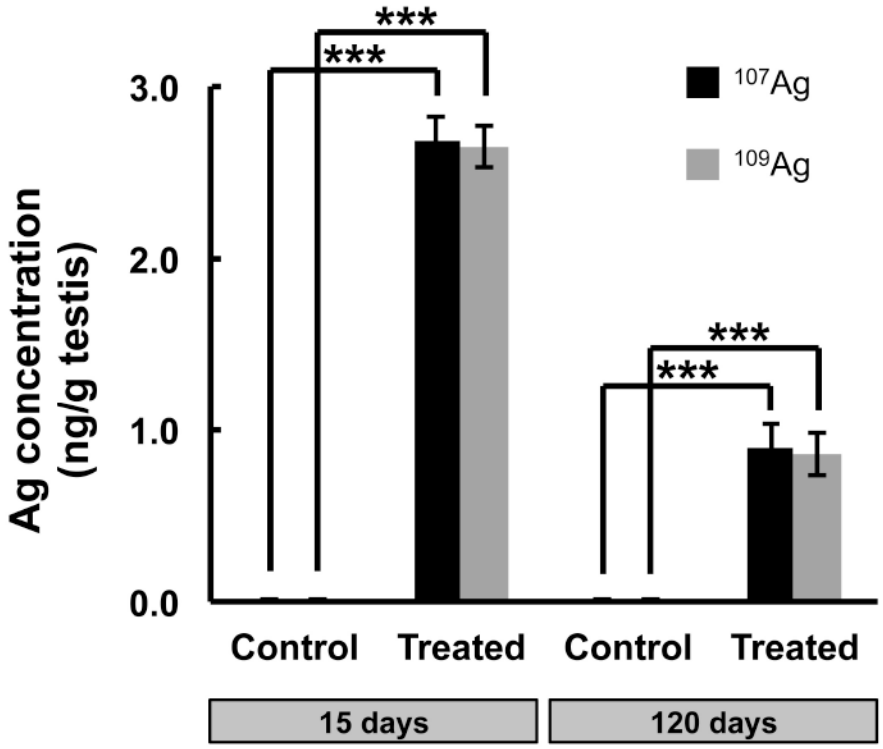

Figure 4.

Silver concentration in testes. Silver concentrations (mean ± SEM, *n*=3) in mouse testes at 15 days post-initial treatment. Statistically significant differences ($P < 0.001$) between the groups are marked with asterisks (***).

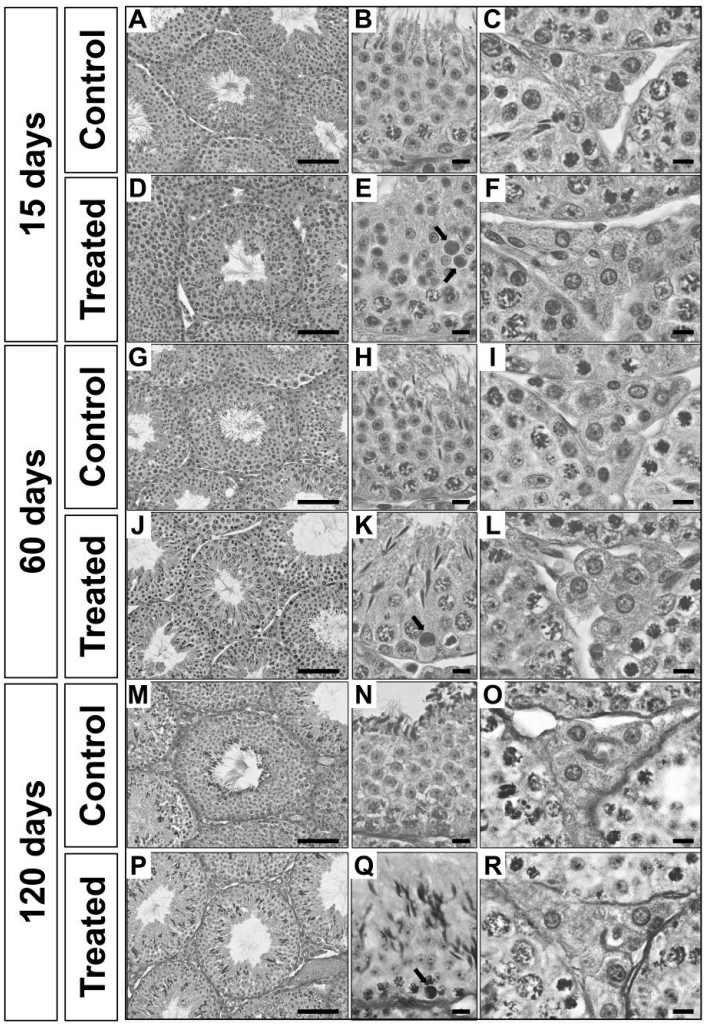

Figure 5.

Light microscopy images of testis sections from control and treated mice at the indicated time points. Treated mice received five doses of nanoparticles (1 mg/kg/dose) and were sacrificed 15 (Panels D, E and F), 60 (Panels J, K and L) and 120 (Panels P, Q and R) days after the first injection. As illustrated in the higher magnification panels (Panels E and K), tubular cross-sections of seminiferous epithelium show that treated mice present a significant increase in germ cell apoptosis. Regarding the Leydig cell morphology, as depicted in the higher magnification panels, treated mice (Panels F, L and R) present higher Leydig cell volume when compared to control mice (Panels C, I and O). Scale bars from panels A, D, G, J, M and P represent 100 μm and scale bars from panels B, C, E, F, H, I, K, L, N, O, Q, R represent 10 μm. Arrows (Panels E and K) are indicating apoptotic cells.

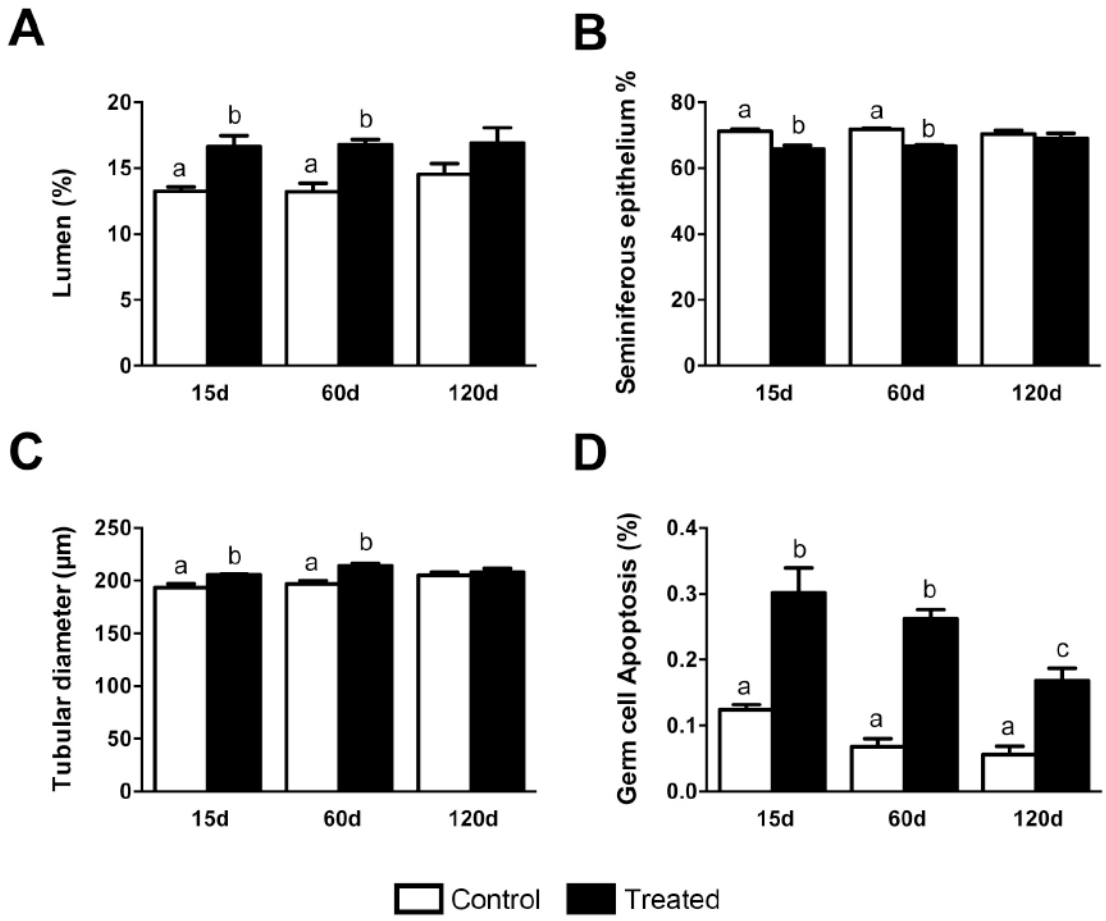

Figure 6.

Morphological alterations of the tubular compartment of mouse testis at 15, 60 and 120 days after silver nanoparticles treatment. The main morphological alterations in the tubular compartment occurred at 15 and 60 days after silver nanoparticles treatment. (A) The lumen volume density was significantly increased ($P<0.05$); (B) seminiferous epithelium volume density was significantly decreased ($P<0.05$); and (C) a significant increase ($P<0.05$) in tubular diameter was also observed in treated groups. The germ cell apoptosis (D) were significantly increased ($p<0.05$) in all time periods evaluated when compared to the control group. Data are presented as mean ± standard error of mean (SEM). Statistical analysis was performed using one-way ANOVA. Letters denote post-hoc test differences.

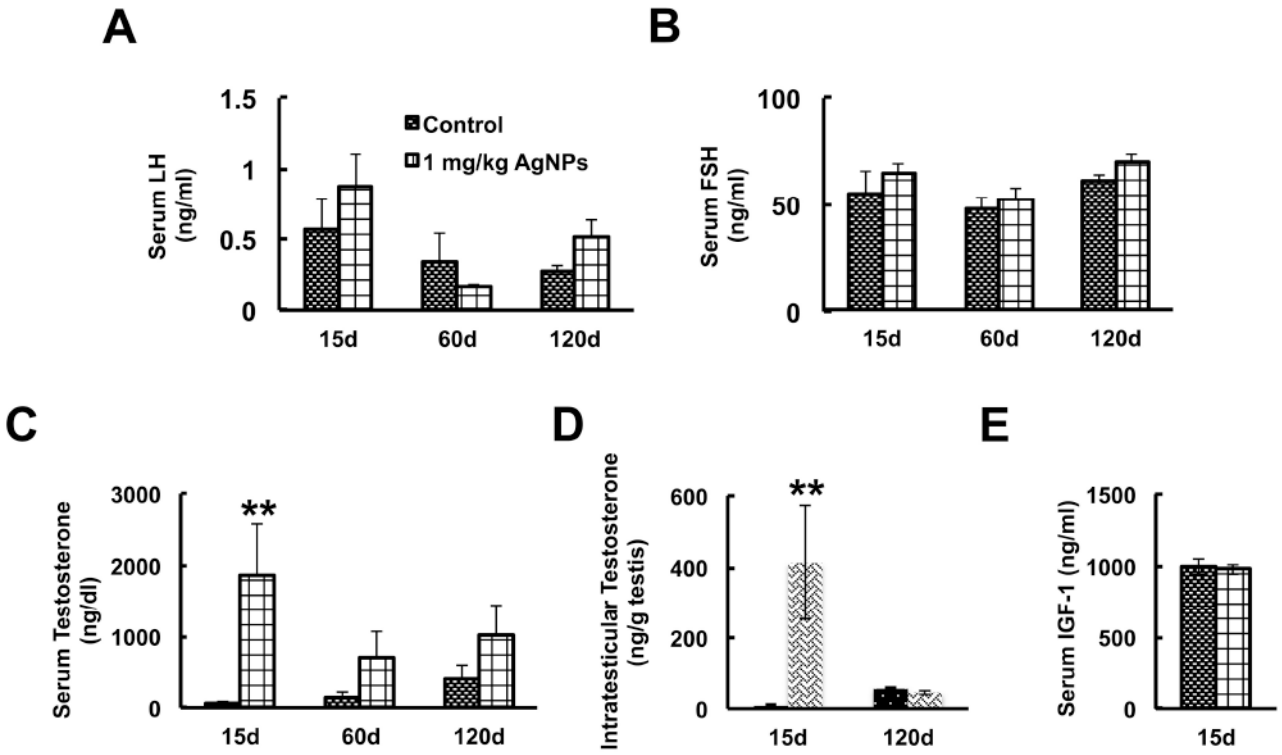

Figure 7.

Serum and intratesticular levels of testosterone in AgNP-treated animals.

The graphs show serum luteinizing hormone (LH) (Panel A), follicle stimulating hormone (FSH) (Panel B), serum testosterone (Panel C) levels, intratesticular testosterone (Panel D), and serum IGF1 (Panel E) levels at the indicated time points post-initial exposure. Serum LH, FSH, and IGF1 were not significantly altered by AgNP treatment; however, serum and intratesticular testosterone were significantly elevated at 15 days post-initial exposure. Statistical analysis was performed using one-way ANOVA (A-D) or Student's *t*-test (E). $n=12$; $^{**}P<0.05$.

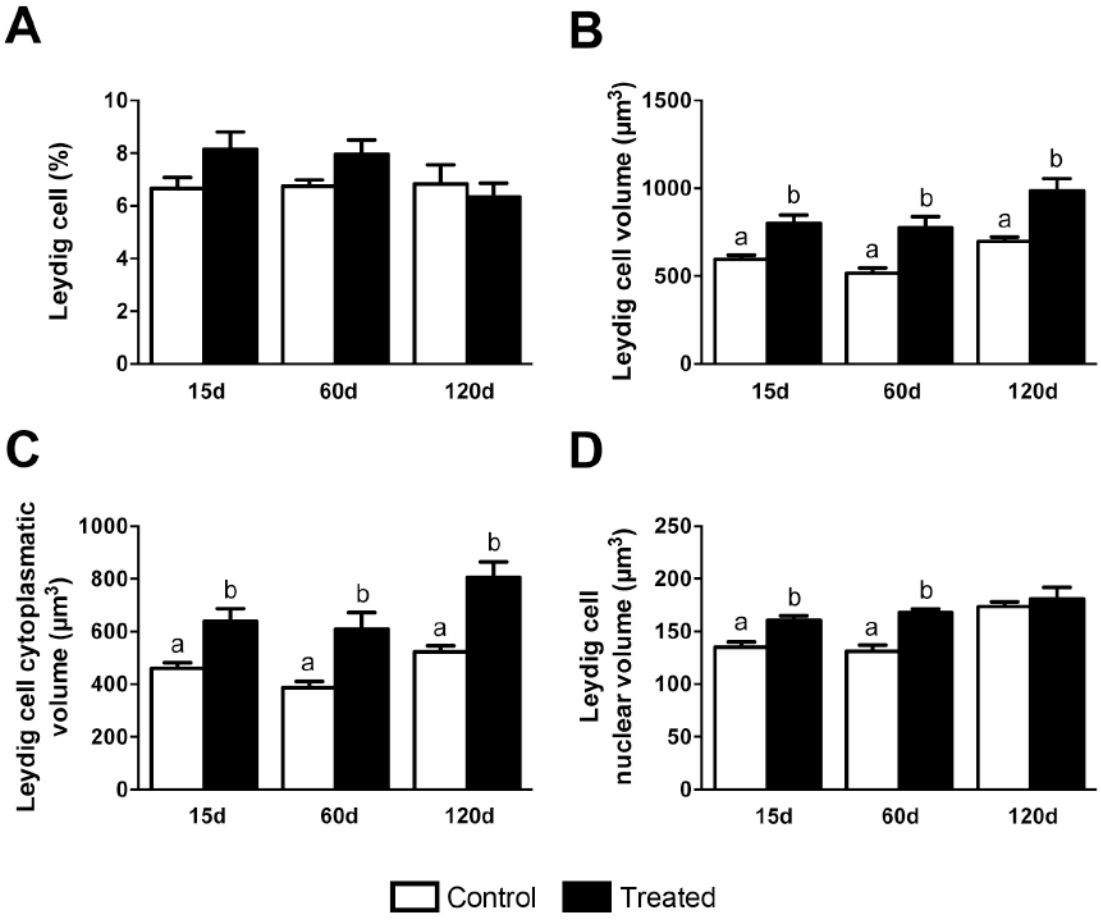

Figure 8.

Morphological alterations of mouse Leydig cells at 15, 60 and 120 days after silver nanoparticles treatment. Although the Leydig cell volume density (A) and their number per testis (B) were similar among control and treated groups, the nuclear (C) and the cytoplasmatic (D) volume of Leydig cells were significantly higher ($P<0.05$) in mice treated with silver nanoparticles. As a consequence, the Leydig cell volume/size (E) significantly increased ($P<0.05$) in treated mice. Data are presented as means ± standard error of mean (SEM). Statistical analysis was performed using one-way ANOVA. Letters denote post-hoc test differences.

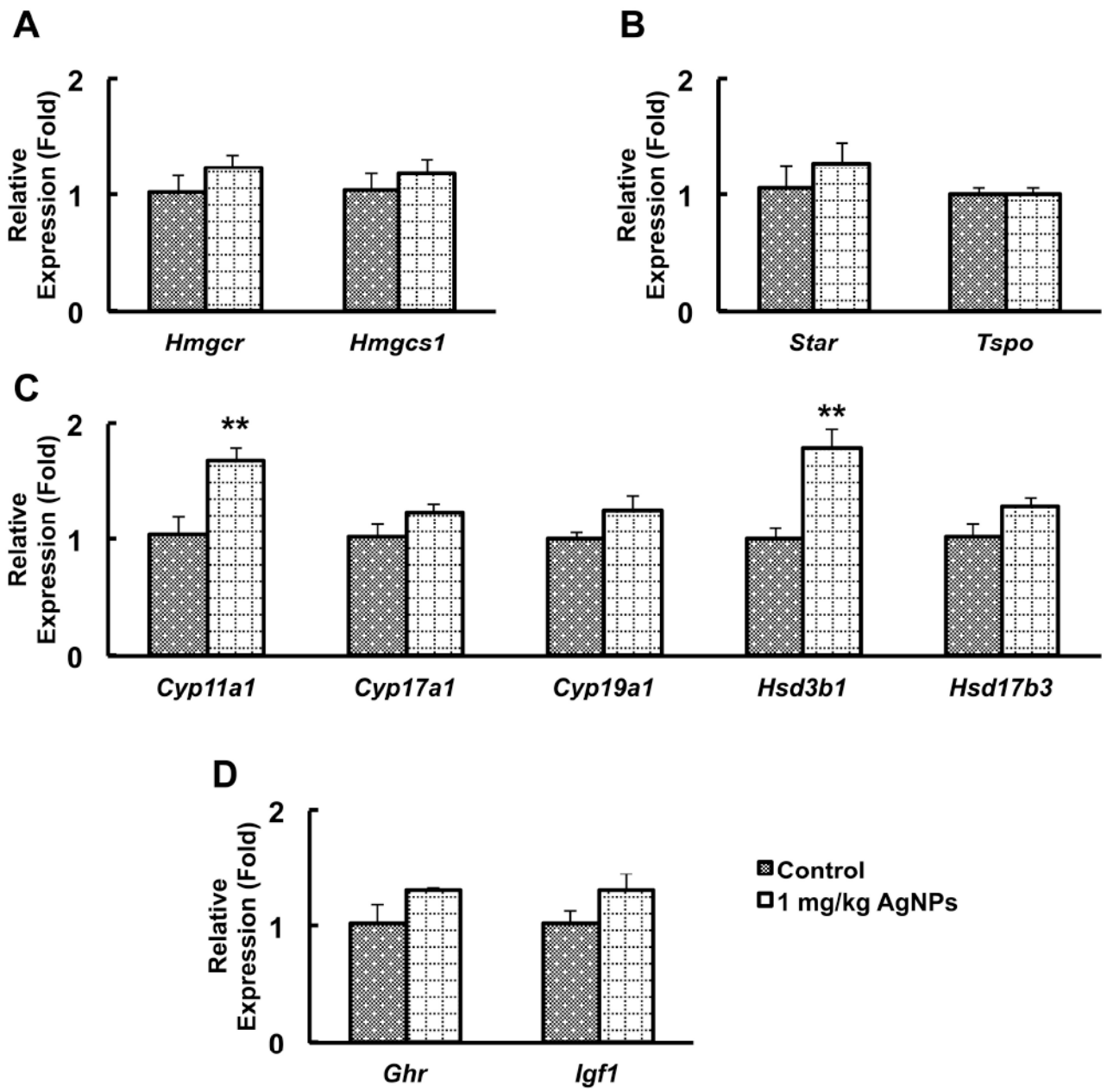

Figure 9.

Testis gene expression analysis of cholesterol biosynthesis, cholesterol transport, testosterone and estradiol biosynthesis, and growth hormone (GH)-related genes

Panels A-D show real-time polymerase chain reaction analysis of cholesterol biosynthesis (Panel A), cholesterol transport (Panel B), testosterone and estradiol biosynthesis (Panel C), and GH and IGF1 signaling-related genes (Panel D) in whole testes of untreated and treated mice at 15 days post-initial exposure. Results are given as mean ± standard errors of means (SEMs). Statistical analysis was performed using Student's *t*-test. $n=6$; $^{**}P<0.05$.

Table I

Sperm parameters as established by computer-assisted sperm analysis.

	Day 15		Day 60		Day 120	
Parameter	**Control (mean ± SEM)**	**AgNP (mean ± SEM)**	**Control (mean ± SEM)**	**AgNP (mean ± SEM)**	**Control (mean ± SEM)**	**AgNP (mean ± SEM)**
Smoothed path velocity (VAP) (μm/s)	115.68±9.04	118.42±6.18	134.93±6.89	109.38±9.06	117.43±4.39	116.6±3.84
Straight line velocity (VSL) (μm/s)	87.38±8.76	90.08±5.83	97.23±6.50	72.88±8.02	80.03±2.98	81.48±2.85
Track velocity (VCL) (μm/s)	208.14±13.12	219.28±8.55	240.23±9.69	202.83±12.98	223.52±5.46	221.28±4.83
Amplitude of lateral head displacement (ALH) (μm)	11.1±0.53	10.92±0.37	13.33±0.35	11.9±0.56	13.17±0.31	13±0.27
Beat cross frequency (BCF) (Hz)	29.74±0.64	32.86±1.70	25.83±0.73	28.28±1.06	28.58±1.19	28.47±1.32
Straightness (STR) (VSL/VAP)	71.2±1.77	70.8±1.46	69.25±1.25	63.5±2.40	65.33±0.56	66.83±0.91
Linearity (LIN) (VSL/VCL)	42.4±1.29	41.2±1.24	40.5±1.32	36.25±2.17	35.83±0.65	37±0.89
Elongation/Head shape (ratio of minor to major axis of sperm head)	43±0.63	42.8±0.86	42.25±0.75	46.25±1.84	43.67±0.42	42.67±0.80
Total (millions/ml)	16.22±2.16	11.62±1.62	28.63±1.89	36.43±4.21	35.32±2.35	31.17±4.00
Motile (%)	77.4±3.64	74.2±4.75	85.5±2.87	87.5±1.55	83.17±1.49	81.17±1.78
Progressive (%)	53.8±3.26	49.0±5.37	62.0±3.19	54.0±3.70	52.67±1.12	52.5±2.33
Rapid (%)	67.8±3.68	63.4±5.22	77.5±3.01	76.5±3.01	71.33±1.38	68.67±2.25
Slow (%)	1.6±0.24	2.2±0.58	1.25±0.25	1.5±0.29	1.33±0.21	1.83±0.17
Static (%)	20.8±3.57	23.6±4.35	13.5±2.87	11.25±1.44	15.3±1.52	17.17±1.70

Table II

Pregnancy rate and number of fetuses in female mice mated with treated males.

	Day 15		Day 60		Day 120	
	Control	**AgNP**	**Control**	**AgNP**	**Control**	**AgNP**
Number of females mated	12	12	12	12	12	12
Number of females preganant	12	11	10	12	12	12
Average number of fetuses per pregnant female	14.1±0.48	13.3±0.54	11.6±0.61	12.1±1.18	11.7±0.37	11.6±0.81